

Bonding and XPS chemical shifts in ZrSiO_4 versus SiO_2 and ZrO_2 : Charge transfer and electrostatic effects

M. J. Guittet,¹ J. P. Crocombette,² and M. Gautier-Soyer^{1,*}

¹DSM/DRECAM/SPCSI-CEA Saclay, 91191-Gif sur Yvette Cedex, France

²DTA/DECM/SRMP-CEA Saclay, 91191-Gif sur Yvette Cedex, France

(Received 4 February 2000; revised manuscript received 26 September 2000; published 13 March 2001)

The degree of ionic/covalent character in oxides has a great influence on the electronic structure and the material's properties. A simple phenomenological rule is currently used to predict the evolution of covalence/ionicity in mixed oxides compared to the parent ones, and is also widely used to interpret the x-ray photoelectron spectroscopy (XPS) binding-energy shifts of the cations in terms of charge transfer. We test the validity of this simple rule and its application to XPS of mixed oxides with a prototypical system: zircon ZrSiO_4 and parent oxides ZrO_2 and SiO_2 . The ionic charges on Si, Zr, and O were extracted from the density functional theory in the local density approximation calculations in the plane-wave formalism. In agreement with the predictions of the phenomenological rule, the most ionic cation (Zr) becomes more ionic in ZrSiO_4 than in ZrO_2 , while the more covalent one (Si) experiences a corresponding increase in covalence with respect to SiO_2 . The XPS chemical shifts of the O $1s$, Si $2p$, and Zr $3d_{5/2}$ photoelectron lines in the three oxides were measured and the respective contributions of charge transfer and electrostatic effects (initial state), as well as extra-atomic relaxation effects (final state) evaluated. The validity of the phenomenological rule of mixed oxides used in x-ray electron spectroscopy as well as the opportunity to use the O $1s$ binding-energy shifts to derive a scale of covalence in silicates is discussed.

DOI: 10.1103/PhysRevB.63.125117

PACS number(s): 82.80.Pv, 71.15.Mb, 71.20.Ps

I. INTRODUCTION

The degree of ionic and covalent character in the bonding of metal oxides has a great influence on the electronic structure and the material's properties. In the case of mixed oxides (e.g., oxides containing more than one type of cation), there remains much to understand as to the amount of ionic/covalent character compared to the simple oxides. One can expect that x-ray photoelectron spectroscopy (XPS) chemical shifts could help to elucidate the bonding character, provided they are correctly interpreted. In this respect, interesting trends in the bonding in superconducting oxides have been reported from the cation chemical shifts.¹ More generally, based on XPS measurements, a phenomenological view of bonding in mixed oxides has been given by Barr,² which states as follows. Considering the mixing of two oxides (A_mO_n and M_xO_y) to form a complex mixed oxide ($A_zM_sO_t$), the cation (A) of the more ionic metal oxide (e.g., A_mO_n) is expected to become even more ionic after formation of the complex oxide, whereas the cation (M) of the more covalent oxide (M_xO_y) should experience a corresponding increase in covalence. In other terms, this means that the charge on the A cation is expected to be larger in the mixed oxide than in the A_mO_n oxide, while the charge of the M cation is expected to be smaller than in the M_xO_y oxide. The atomic charges on the atoms are not directly measurable, and core-level XPS chemical shifts, which reflect this evolution in the cation charges, can be of great use. Such an approach has been successfully used in catalysis and in the study of the acidity of complex aluminosilicate compounds such as zeolites.³ However, to the best of our knowledge, no theoretical proof for this general empirical rule has been reported yet.

We chose to test this rule on a prototypical system: zircon ZrSiO_4 , which is of interest in the field of nuclear materials, and two parent oxides monoclinic zirconia ZrO_2 and α -quartz SiO_2 . This is an interesting system, as the formal valences of Zr and Si are the same in the simple and mixed oxides (+4). The purpose of this paper is twofold.

(1) On the theoretical side, we have used *ab initio* electronic structure calculations to derive the atomic charges in an attempt to check if the empirical rule was verified in this particular case.

(2) On the experimental side, we have measured the shifts of x-ray photoelectron lines characteristic of cations and oxygen. The relative importance of the different contributions has been estimated: charge transfer (fingerprint of covalence/ionicity), Madelung potential (representing the electrostatic interaction between the probed atom and its neighbors), which are both characteristic of the initial state, as well as the relaxation effects (final state). Then we have discussed these shifts in terms of the balance between covalence/electrostatic effects in the initial state in the frame of the picture of bonding given by the *ab initio* atomic charge calculations.

Quantum mechanical methods especially devoted to the determination of XPS core-level chemical shifts have been developed in the last years.⁴ Such methods are up to now performed on clusters, and very efficient in molecules, in which the binding energies are calculated with an accuracy comparable to the experimental values (0.2 eV),⁵ but these methods are not exempt from finite-size effects.⁶

In the present work, we have chosen a simple approach based on the well-known formula generally put forward to estimate the XPS chemical shifts $\Delta E_b(A)$ between a free atom and an atom in an oxide.⁷ This formula is in the form of a linear relationship between the atomic charge q_A , the

Madelung energy Mad_A , and relaxation energy E_A^{rel} :

$$\Delta E_b(A) = kq_A + \text{Mad}_A + E_A^{\text{rel}}. \quad (1)$$

The contribution ($kq_A + \text{Mad}_A$) to the measured chemical shift arises from initial-state effects and reflects the initial-state chemistry. The last term E_A^{rel} is related to final-state effects that arise from the charge rearrangement or relaxation that occurs in response to the core hole.

More precisely, k is related to the interactions experienced by the core state as a result of the changes (between the free atom and the oxide) induced into the valence shell of the A atom. In fact, there are nonlinear terms in the charge-transfer contribution that can be modeled effectively by giving k a dependence on both the valence charge and the degree of core ionization.^{8,9} However, these effects have not yet been taken into account in the case of oxides, and this may limit the accuracy of the present results.

The Madelung energy for an electron of atom A is written within the assumption that the neighboring atoms can be assimilated to point charges, which neglects the polarization of the ions,

$$\text{Mad}_A = - \sum_{B \neq A} \frac{q_B}{r_{A-B}}, \quad (2)$$

where q_B denotes the charges of the other atoms and r_{A-B} the interatomic distances. For a given atom A in two different materials, one can write

$$\Delta E_b(A) = k\Delta q_A + \Delta \text{Mad}_A + \Delta E_{\text{ca}A}^{\text{rel}}, \quad (3)$$

where $\Delta E_{\text{ca}A}^{\text{rel}}$ is the difference in the extra-atomic part of the relaxation energy, as the intra-atomic part of it is not changed.

If A is a cation and if one could neglect Madelung and relaxation effects in the above formula (3), an increased ionicity would lead to an increase in the cation binding energy, while an increased covalence would lead to a decrease of it.

In fact, initial-state effects often make the dominant contributions to the binding-energy shifts.^{4,10} But this is an oversimplification of considering charge transfer as the dominant mechanism for binding-energy shifts and considering that $\Delta E_b(A)$ is simply proportional to Δq_A . Indeed, it has been shown that in some cases the Madelung contribution can be of fundamental importance. More precisely, a simple interpretation of the O $1s$ chemical shifts as reflecting only the charge transfer along the series MgO-CaO-SrO-BaO leads to the false conclusion that MgO is less ionic than BaO. It is the variation of Madelung potentials arising from changes in the interatomic distance r_{O-M} along the series that holds the key to understanding the chemical shifts.⁶ Then, every contribution to the chemical shifts can be relevant and none of these can be *a priori* ignored.

In the present work, the XPS binding energies as well as the variation in the extra-atomic relaxation energies have been measured in the same spectrometer (Sec. II), while the atomic charges q_A as well as the related Madelung energies Mad_A have been calculated thanks to an *ab initio* density functional method (Sec. III) for $A = \text{Zr}$, Si, and O. In Sec. IV,

the measured binding energies of cations and oxygen in the mixed oxide are discussed with respect to the simple oxides already stated. Eventually, the validity of the Barr phenomenological rule of mixed oxides² is discussed in the present system along with the opportunity to use the O $1s$ shifts to derive a scale of covalence of silicates.

II. EXPERIMENT

The samples used were SiO₂ and ZrSiO₄ powders pressed onto an indium foil. ZrO₂ powder was a sintered pellet heated up to 1500 °C to ensure stoichiometry. The XPS analyses were performed in a VG ESCALAB Mark II. X-ray photoelectron spectra were produced using a nonmonochromatized x-ray source ($h\nu = 1486.6 \text{ eV}$). Calibration of the spectrometer was such that the Ag $3d_{5/2}$ line had a binding energy of 368.35 eV. Survey spectra were recorded for the 0–1250 eV region to determine the elements present in the sample and to check for surface contamination. Then the O $1s$, Zr $3d$, and Si $2p$ photoelectron lines, as well as the O KLL, Zr LMM, and Si KLL Auger lines were recorded. Figure 1 displays the (a) O $1s$, (b) Si $2p$, and (c) Zr $3d$ photoelectron lines. Their intensity is normalized at the maximum of the line. The Auger parameters A'_O , A'_{Si} , and A'_{Zr} were calculated according to

$$A'_O = E_b(\text{O } 1s) + E_{\text{kin}}(\text{O KLL}),$$

$$A'_{\text{Si}} = E_b(\text{Si } 2p) + E_{\text{kin}}(\text{Si KLL}),$$

$$A'_{\text{Zr}} = E_b(\text{Zr } 3d_{5/2}) + E_{\text{kin}}(\text{Zr LMM}).$$

From these parameters one can deduce the variation of the extra-atomic relaxation energy $\Delta E_{\text{ca}}^{\text{rel}}$ as it has been shown to be half the variation of the Auger parameter.^{11,12}

All three materials are insulating, so that surface charging has to be taken into account to derive absolute binding energies. However, if there is no differential charging, the Auger parameter values (kinetic-energy differences) are independent of charging. Their values are given in Table I. With a nonmonochromatic x-ray source (this work), the Al window which shields the sample from energetic electrons emitted by the anode, acts itself as a source of low-energy secondary electrons so that a charge equilibrium is achieved. However the point of stable surface potential does not correspond to the ground potential of the spectrometer. It is then necessary to have some internal reference peak within the spectrum that may be used to correct the spectrum to the reference binding-energy scale. The C $1s$ line of adventitious carbon is most commonly used for this purpose: the true binding energy for a photoelectron line is assumed to be $E_b - V$, where E_b is the measured binding energy and V is the correction term due to charging, which is the difference between the surface potential and the spectrometer ground potential. This procedure assumes that (i) the differential charging is negligible so that the entire spectrum is uniformly shifted by the

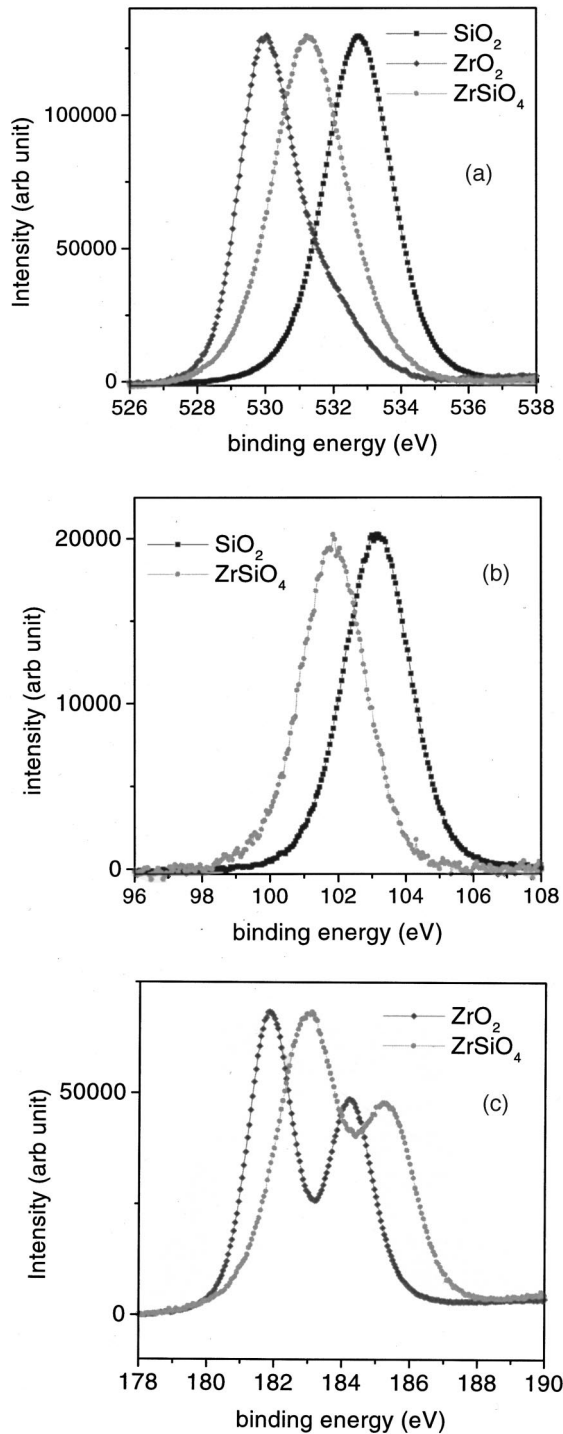


FIG. 1. Photoelectron lines of SiO₂, ZrO₂, and ZrSiO₄. The (a) O 1s, (b) Si 2p, and (c) Zr 3d photoelectron lines are normalized in intensity at the maximum of the peak. See text for energy calibration.

constant energy V and (ii) the C 1s line of adventitious carbon is of the same kind for the materials we wish to compare together.

To ascertain assumption (ii), we have checked that the C 1s photoelectron lines of our three samples have similar shape and width between 2.1 and 2.4 eV. To ascertain as-

sumption (i), we have compared the Auger parameters as well as oxygen/cation binding-energy differences with those obtained in our previous work of Ref. 13. The aim of this previous work, carried out with a monochromatic Al $K\alpha$ x-ray source, was to determine the best procedure to overcome the charging effects by using a low-energy electron flood gun.¹³ With SiO₂ and ZrO₂ single crystals, we had measured, as a function of the energy of flooding electrons, the binding energy of the O 1s, Si 2p, and Zr 3d_{5/2} lines as well as their full width at half maximum (FWHM). It turned out that the real criterion for the optimization of the flood gun was not the energy position of the lines but more likely the lowest FWHM for the highest intensity, both parameters having to be examined simultaneously. Optimization was thus achieved when the charge was “overcompensated,” i.e., the sample was negatively charged.

The A'_O values recorded on ZrO₂ and SiO₂ single crystals, under the experimental conditions of Ref. 13, are also written in Table I along with the width of the O 1s, Si 2p, and Zr 3d_{5/2} photoelectron lines. The oxygen Auger parameter A'_O obtained with the ZrO₂ powder in the present work is quite in accordance with the values obtained for the ZrO₂ single crystal.¹³ However, the A'_O value is smaller for the present SiO₂ powder than for the single crystal of Ref. 13. This can be due to a slight charging effect, as we had observed that the A'_O value on the single crystal was decreased when the energy of the flooding electrons was close to 0 eV. However, the binding-energy differences $E_b(\text{O } 1s) - E_b(\text{Si } 2p) = 429.5$ eV and $E_b(\text{O } 1s) - E_b(\text{Zr } 3d_{5/2}) = 348.1$ eV are the same in the present work and in Ref. 13. As concerns the FWHM of the photoelectron lines, the O 1s and Zr 3d_{5/2} FWHM of the present work agree very well with the values obtained for the ZrO₂ single crystal in Ref. 13. For the SiO₂ powder the FWHM of the O 1s and Si 2p peaks are slightly larger than for the SiO₂ single crystal, but this broadening is more likely due to the amorphous state of the powder than to the charging effect. In addition, the O 1s and Si 2p binding energies as well as the A_{Si} Auger parameter are in accordance with the values gathered by Wagner *et al.*¹⁴

To sum up, the width of the peaks as well as the binding-energy differences are in good agreement with the values obtained from a systematic study with a monochromatic source operated with a flood gun on single crystals.¹³ Differential charging can be assumed to be negligible. Calibration was thus achieved by setting the C 1s binding energy at 284.6 eV, which is the value measured in our spectrometer on a very thin carbon contamination layer on metallic samples. The binding energies measured using this procedure are reported in Table I.

III. CHARGE CALCULATIONS

The charges borne by the ions in the three oxides have been extracted from *ab initio* electronic-structure calculations based on the density-functional theory in the local density approximation (DFT-LDA). These calculations were primarily done to study structural and defect properties of zircon and α -quartz.^{15–17} For what concerns the crystallographic structure of these materials, silicon atoms exhibit the

TABLE I. Measured binding energies of the O $1s$, Zr $3d_{5/2}$, and Si $2p$ photoelectron lines in SiO_2 , ZrSiO_4 , and ZrO_2 , as well as O, Zr, and Si Auger parameters deduced from the above binding energies and the kinetic energies of the O KLL , Zr LMM , and Si KLL Auger lines in the same oxides. All values are in eV.

Oxide	$E_b(\text{O } 1s)$	A'_O	$E_b(\text{Zr } 3d_{5/2})$	A'_{Zr}	$E_b(\text{Si } 2p)$	A'_{Si}
SiO_2	532.7 ($W=2$)	1039.14			103.15 ($W=2$)	1711.9
ZrSiO_4	531.3 ($W=2.3$)	1040.3	182.95 ($W=1.8$)	2015	101.8 ($W=2$)	1713.1
ZrO_2	530 ($W=1.4$)	1040.85	181.9 ($W=1.4$)	2015.2		
SiO_2 single crystal ^a	($W=1.6$)	1039.7			($W=1.7$)	
ZrO_2 single crystal ^a	($W=1.6$)	1040.95	($W=1.4$)			

^aExperiments performed with a monochromatized Al $K\alpha$ source, on single crystal following the experimental procedure described in Ref. 7. The differences in binding energies were $E_b(\text{O } 1s) - E_b(\text{Si } 2p) = 429.5$ eV (against 429.55 eV in this work) and $E_b(\text{O } 1s) - E_b(\text{Zr } 3d_{5/2}) = 348$ eV (against 348.1 eV in this work)

same SiO_4 tetrahedra in quartz and zircon whereas seven neighbors in monoclinic zirconia versus eight in zircon surrounding zirconium atoms. The oxygen atoms are tricoordinated with one Si and two Zr atoms in zircon, while they have two silicon neighbors in SiO_2 and four Zr neighbors in monoclinic zirconia.

We used the plane-wave self-consistent field code¹⁸ that deals with a plane-wave basis, the pseudopotentials, of the norm-conserving type, were the same as the ones considered in our previous study on zircon structure¹⁶ to which the reader is invited to refer to for technical details. The calculations were made on the numerically relaxed atomic structure for zircon and α -quartz. To save computational time we considered for zirconia the experimental monoclinic structure. We chose a value of 95 Ry for the energy cutoff in the plane-wave expansion. Such a high value is needed to correctly take into account the zirconium atoms. It also provides a tight mesh of points in real space, which proves important for the calculation of the ionic charges. Indeed the calculated charge density comes out of the calculation as a distribution over a real space grid of equally spaced points. Due to the high cutoff, we reached a density of points of approximately 3000 points per \AA^3 .

Many subtle procedures exist to estimate atomic charges from quantum mechanical calculations. Some, like the Mulliken population analysis,¹⁹ presuppose the use of an atomic-orbital basis set and are thus not applicable within a plane-wave basis. Others require knowing charge clouds around the free atomic species.^{20,21} Such methods can be adapted to plane-wave calculations at the expense of additional calculations. We chose to work directly on the calculated density map as they come out of the DFT calculation. To calculate the ionic charges, one then has to distribute the electronic-charge cloud over the atoms. Quite involved methods based on the analytical properties of the charge distribution exist to do so, see, for instance, Ref. 22. We chose to test a simpler method that can be very easily implemented as a post processing analysis of any DFT calculation. The crystal unit cell was divided into Voronoi cells centered on each nucleus, the

charge contained in each cell was calculated by summing the charge density of all grid points contained in the cell and attributed to the ion contained in the cell. In other words, the charge borne by a mesh point was attributed to the atom closer to this mesh point. Due to the tight mesh we used, it was not necessary to use any smoothing or extrapolation function for the charge density. Indeed this point-by-point method gave the same charges for distinct but crystallographically equivalent atoms with a relative precision better than 1%. From these charges, Madelung energies were calculated by a standard Ewald summation technique.

The charges calculated around each ion in the three crystals are indicated Table II, together with Madelung energies. One can see that the calculated charges are quite meaningful. For instance, zirconia is found to be more ionic than quartz as expected, the oxygen charge being larger in zirconia than in quartz.

IV. DISCUSSION

A. Cations

ZrSiO_4 is a mixed oxide in which Zr is the more ionic cation and Si the more covalent one. Indeed, zirconia ZrO_2 is more ionic than quartz SiO_2 . Table II shows that the calculated charge on Si is smaller in zircon than in quartz, so Si is more covalent in the former than in the latter. On the other hand, the calculated charge on Zr is larger in zircon, so Zr is more ionic in zircon than in zirconia. Coming back to the

TABLE II. Calculated charges on O, Si, and Zr and Madelung energies (in eV) for the electrons of the O, Si, and Zr atoms for the three oxides SiO_2 , ZrSiO_4 , and ZrO_2 .

Oxide	q_O	q_{Si}	q_{Zr}	Mad_O	Mad_{Si}	Mad_{Zr}
SiO_2	-1.02	2.05		-15.26	23.32	
ZrSiO_4	-1.19	1.93	2.85	-15.84	25.49	28.37
ZrO_2	-1.38		2.76	-16.27		29.52

TABLE III. Different contributions to the XPS measured binding-energy shifts for the cations ($A = \text{Si}, \text{Zr}$). For Si, the energy reference is the value in SiO₂, while for Zr, it is the value in ZrO₂. All values are in eV. In the first column, $\Delta E_b(A)$ are the measured XPS chemical shifts of the Si $2p$ and Zr $3d_{5/2}$ photoelectron lines in ZrSiO₄. The second column gives the difference in the calculated Madelung energies (cf. Table II). In the third one are the differences in the extra-atomic relaxation energies (deduced from Table I). The fourth column gives the charge-transfer contribution derived from these values following Eq. (3), and the last column gives the differences in the calculated charges (cf. Table II).

	$\Delta E_b(A)$ measured	ΔMad_A calculated	$\Delta E_{\text{ea}A}^{\text{rel}}$ measured	$k\Delta q_A$	Δq_A calculated
Si in ZrSiO ₄	1.35	-2.17	-0.6	4.12	0.12
Zr in ZrSiO ₄	-1.05	+1.15	+0.1	-2.3	-0.09

phenomenological rule of mixed oxides given by Barr,² the expected behavior of charges is confirmed by the electronic-structure calculation.

As concerns the measured binding energies of the Si $2p$ and the Zr $3d_{5/2}$ photoelectron lines, $E_b(\text{Si})$ is smaller in ZrSiO₄ than in SiO₂, while $E_b(\text{Zr})$ is larger in ZrSiO₄ than in ZrO₂ (Table I). Hence, the binding energy varies in the same way as the cation charges.

Besides the measured binding-energy shifts $\Delta E_b(A)$ and relaxation energy variations $\Delta E_{\text{ea}A}^{\text{rel}}$ given in Table III, the calculated Δq_A and ΔMad_A values for $A = \text{Zr}$ and Si are also reported. From the $\Delta E_b(A)$, ΔMad_A , and $\Delta E_{\text{ea}A}^{\text{rel}}$ values, the so-called $k\Delta q_A$ charge transfer contribution can be derived using Eq. (3). A careful examination of Table III shows that while the relaxation energy variation is negligible for Zr $3d$, this is not the case for Si $2p$. Moreover, the Madelung contribution variation is not negligible at all in both cases. The $k\Delta q_A$ value has the same sign as the binding-energy shift. However, it is about three times larger for Si and two times larger for Zr because the ΔMad_A and $\Delta E_{\text{ea}A}^{\text{rel}}$ values (the absolute values of which are, respectively, about 50% and >15% (5%) of $|k\Delta q_A|$) have the opposite sign. Finally, the more important contribution to the binding-energy shifts of the cations in ZrSiO₄ compared to the simple oxides ZrO₂ and SiO₂ is the charge-transfer contribution $k\Delta q_A$, so that the measured binding-energy shift reflects the charge changes induced by the mixing of oxides with different valencies, the more covalent cation (Si) becoming more covalent, and the more ionic cation (Zr) becoming more ionic. So with the present system, Barr's empirical rule for bonding in mixed oxides is verified theoretically and a crude interpretation of the cation binding-energy shifts in terms of changes in charge transfer would have led to a conclusion qualitatively correct. However the measured effects are limited by the contribution of Madelung and relaxation effects, which are smaller but not negligible at all.

B. Oxygen

Common to all three materials, oxygen is a very important element as its ionic charge is characteristic of the oxide co-

TABLE IV. Different contributions to the XPS measured binding-energy shifts for oxygen. The energy reference is the value for SiO₂. All values are in eV. In the first column, $\Delta E_b(\text{O})$ are the measured XPS chemical shifts of the O $1s$ photoelectron line in ZrSiO₄ and ZrO₂. The second column gives the difference in the calculated Madelung energies (cf. Table II). In the third one are the differences in the extra-atomic relaxation energies (deduced from Table I). The fourth column gives the charge-transfer contribution derived from these values following Eq. (3), and the last column gives the differences in the calculated charges (cf. Table II).

	$\Delta E_b(\text{O})$ measured	$\Delta \text{Mad}_\text{O}$ calculated	$\Delta E_{\text{eaO}}^{\text{rel}}$ measured	$k\Delta q_\text{O}$	Δq_O calculated
O in ZrSiO ₄	1.4	-0.58	+0.58	1.4	0.17
O in ZrO ₂	2.7	-0.85	1.01	2.54	0.36

valence so that comparison of the oxygen charges in different oxides would then make it possible to build a covalence scale. Unfortunately, these charges are not directly measurable. Then, assuming that the O $1s$ binding-energy shifts could be crudely interpreted in terms of changes in the oxygen ionic charge, it was proposed to use these measured binding-energy shifts as a probe of the covalence/ionicity of oxides and some attempts have been made previously to correlate the XPS oxygen chemical shifts to the Pauling oxygen charge in oxides.²³ However, as pointed out in Sec. I, such an approach can be misleading if the charge-transfer contribution is not the leading contribution to the measured binding-energy shift.⁶

The calculated oxygen charges of Table II give for ZrSiO₄ a q_O value intermediate between the value in SiO₂ and ZrO₂. Turning to the binding energy of oxygen in the mixed oxide, we obtain as expected, an intermediate value between the values of the simple oxides taken separately (Table I). To relate the chemical shift of the O $1s$ photoelectron line to the calculated charge distributions we have decomposed the measured binding-energy shift into charge transfer, Madelung, and extra-atomic relaxation contributions, very much the same way as for cations in the preceding section by taking the SiO₂ energies as reference (Table IV). The striking feature is that this time $\Delta \text{Mad}_\text{O}$ and $\Delta E_{\text{eaO}}^{\text{rel}}$ are not negligible, but compensate as they have very close values of opposite sign. As a result, the measured binding-energy shift $\Delta E_b(\text{O})$ is equal or very close to the $k\Delta q_\text{O}$ contribution within the 0.2 eV experimental accuracy.

Figure 2 shows the plot of the experimentally measured chemical shift $\Delta E_b(\text{O})$ relative to SiO₂ as well as $k\Delta q_\text{O}$ (including the extra-atomic relaxation and Madelung corrections) as a function of the oxygen charges. A straight line can fit indeed both the measured binding-energy shift $\Delta E_b(\text{O})$ and its corrected value $k\Delta q_\text{O}$ very accurately with "correlation coefficients" of 0.9971 and 0.9964, respectively. This linearity in the present case makes us confident to tentatively use it in the future for more complex mixed oxides based on the SiO₂ matrix. The plot of Fig. 2 could be used as a scale of covalence to deduce from the chemical shift of the O $1s$ line, an estimate of the oxygen charge characteristic of the covalence of more complex silicates. The main feature of the

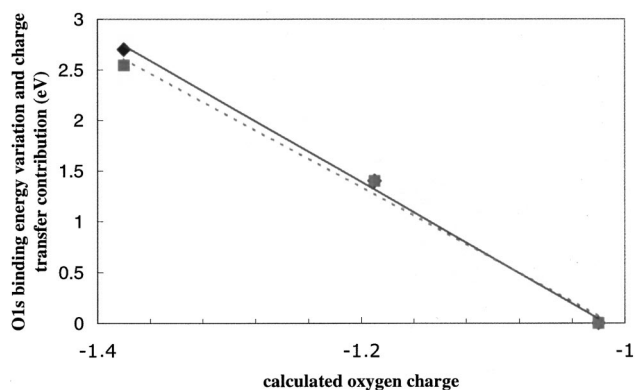


FIG. 2. Evolution of the measured binding energy ΔE_b (O $1s$) of the O $1s$ line (lozenges ges, solid line) and of the charge-transfer contribution $k\Delta q_O$ (squares, dashed line) as a function of calculated oxygen charges in ZrO_2 , $ZrSiO_4$, and SiO_2 . As in Table IV, the reference of the O $1s$ binding energies is the value in SiO_2 .

present work is to use oxygen charges that have been calculated with the same *ab initio* method, and that are expected to give a more realistic electronic description of the solid than the Pauling charges. However, this approach would be fully justified if the Madelung and extra-atomic relaxation contributions compensate as in the present case.

C. Validity of the linear dependence on ionic charges

In the classical formula (3), k can be approximated as $1/\langle r \rangle$, where $\langle r \rangle$ is the radius of the outermost valence shell of the probed atom. In $ZrSiO_4$, when the Si $2p$ level is probed, one finds a k_{Si} value of 34.33 eV, while for the Zr $3d$ level, k_{Zr} is found equal to 25.55 eV. These values lead to radii $\langle r_{Si} \rangle = 0.42 \text{ \AA}$ and $\langle r_{Zr} \rangle = 0.56 \text{ \AA}$ in $ZrSiO_4$, which are reasonable values for ionic radii of Si and Zr. Turning now to oxygen, the k_O value of 8.235 eV for $ZrSiO_4$ leads to a radius $\langle r_O \rangle = 1.75 \text{ \AA}$. This would lead to a Si-O mean distance of 2.17 \AA , and a Zr-O mean distance of 2.31 \AA . When comparing with the crystallographic interatomic distances of 1.63 \AA (Si-O) and 2.25 \AA (Zr-O), our model leads well to a Si-O distance shorter than Zr-O, but the error in the Si-O interatomic distances is about 25% in the Zr-O distance. A better precision cannot be expected. This comes from the fact

that, as stated in Sec. I, there are nonlinear terms in the charge-transfer contribution, so that k depends on the valence charge. These effects have not been taken into account in the present work.

V. CONCLUSION

In this paper we applied simple ideas and methods to the problem of determination of charges and covalencies from core-level XPS measurements. Considering zirconia, quartz, and zircon as a prototype system, we experimentally measured the core-level shifts of Si $2p$, Zr $3d_{5/2}$, and O $1s$ photoelectron lines. From DFT-LDA calculations in the plane-wave formalism we calculated the charges on the atoms by simply dispatching the calculated charge density among the atoms' Voronoi cells. This quite crude but easy method gives very sensitive results.

From the calculated cation ionic charges, the evolution of covalence between simple and mixed oxides is proven to follow the general phenomenological trend stated by Barr. Moreover, for what concerns XPS binding-energy shifts of cations, we found that the leading contribution is the charge-transfer contribution, so that an interpretation of the Si $2p$ and Zr $3d$ binding-energy shifts in terms of Si-increased covalence and Zr-increased ionicity is qualitatively correct even if the Madelung and extra-atomic relaxation contributions are not negligible.

As far as oxygen is concerned, the Madelung and extra-atomic relaxation contributions counterbalance each other, so that the measured O $1s$ binding-energy shift is equal to the charge-transfer contribution. As a consequence, with the present system, one can obtain a linear relationship between the measured binding-energy shift and the calculated oxygen charge. This approach gives theoretical grounds to a future analysis of the covalence of more complex oxides such as silicate glasses. Such a work is in progress and will be the subject of a forthcoming paper.

ACKNOWLEDGMENTS

The authors are grateful to P. Trocellier (CEA Saclay, Laboratoire Pierre Sue, France) for providing them the zircon powder, and to A. Bender (CEA Saclay, DSM/DRECAM/SPCSI) for preparing the zirconia sample.

*Corresponding author. Email address: mgautiersoyer@cea.fr

¹T. L. Barr and C. R. Brundle, Phys. Rev. B **46**, 9199 (1992).

²T. L. Barr, J. Vac. Sci. Technol. A **9**, 1793 (1991).

³T. L. Barr, J. Klinowski, H. He, K. Alberti, G. Muller, and J. A. Lercher, Nature (London) **365**, 429 (1993).

⁴P. S. Bagus, F. Illas, G. Pacchioni, and F. Parmigiani, J. Electron Spectrosc. Relat. Phenom. **100**, 215 (1999).

⁵D. P. Chong and C. Bureau, J. Electron Spectrosc. Relat. Phenom. **106**, 1 (2000).

⁶G. Pacchioni and P. S. Bagus, Phys. Rev. B **50**, 2576 (1994).

⁷D. Briggs and M. P. Seah, *Practical Surface Analysis* (Wiley, Chichester, 1990), p. 420.

⁸R. J. Cole, D. A. C. Gregory, and P. Weightman, Phys. Rev. B

49, 657 (1994).

⁹M. D. Jackson, R. J. Cole, N. J. Brooks, and P. Weightman, J. Electron Spectrosc. Relat. Phenom. **72**, 261 (1995).

¹⁰T. L. Barr, E. Hoppe, T. Dugall, P. Shah, and S. Seal, J. Electron Spectrosc. Relat. Phenom. **98–99**, 95 (1999).

¹¹C. D. Wagner, Anal. Chem. **47**, 1201 (1975).

¹²G. Moretti, J. Electron Spectrosc. Relat. Phenom. **95**, 95 (1998).

¹³F. Bart, M. J. Guittet, M. Henriot, N. Thromat, M. Gautier, and J. P. Duraud, J. Electron Spectrosc. Relat. Phenom. **69**, 245 (1994).

¹⁴C. D. Wagner, D. E. Passoja, H. F. Hillery, T. G. Kinisky, H. A. Six, W. T. Jansen, and I. A. Taylor, J. Vac. Sci. Technol. **21**, 933 (1982).

- ¹⁵Y. Limoge, private communication.
- ¹⁶J. P. Crocombette and D. Ghaleb, *J. Nucl. Mater.* **257**, 282 (1998).
- ¹⁷J.-P. Crocombette, *Phys. Chem. Miner.* **27**, 138 (1999).
- ¹⁸Plane-wave self-consistent field code was obtained via a collaboration with S. Baroni from CECAM (Centre Européen de Calculs Atomiques et Moléculaires).
- ¹⁹R. S. Mulliken, *J. Chem. Phys.* **23**, 1833 (1955).
- ²⁰P. Politzer and R. Harris, *J. Am. Chem. Soc.* **92**, 6451 (1970).
- ²¹F. L. Hishfeld, *Theor. Chim. Acta* **44**, 129 (1977).
- ²²R. Bader, *Acc. Chem. Res.* **8**, 34 (1975).
- ²³H. Noller, J. A. Lercher, and H. Vinek, *Mater. Chem. Phys.* **18**, 577 (1988).